JCTC Journal of Chemical Theory and Computation

Path Integral Simulations of Proton Transfer Reactions in Aqueous Solution Using Combined QM/MM Potentials

Dan Thomas Major, Mireia Garcia-Viloca,† and Jiali Gao*

Department of Chemistry and Supercomputing Insititute, Digital Technology Center, University of Minnesota, Minneapolis, Minnesota 55455

Received October 18, 2005

Abstract: A bisection sampling method was implemented in path integral simulations of chemical reactions in solution in the framework of the quantized classical path approach. In the present study, we employ a combined quantum mechanical and molecular mechanical (QM/MM) potential to describe the potential energy surface and the path integral method to incorporate nuclear quantum effects. We examine the convergence of the bisection method for two proton-transfer reactions in aqueous solution at room temperature. The first reaction involves the symmetrical proton transfer between an ammonium ion and an ammonia molecule. The second reaction is the ionization of nitroethane by an acetate ion. To account for nuclear quantum mechanical corrections, it is sufficient to quantize the transferring light atom in the ammonium ion-ammonia reaction, while it is necessary to also quantize the donor and acceptor atoms in the nitroethane-acetate ion reaction. Kinetic isotope effects have been computed for isotopic substitution of the transferring proton by a deuteron in the nitroethane-acetate reaction. In all computations, it is important to employ a sufficient number of polymer beads along with a large number of configurations to achieve convergence in these simulations.

Introduction

The incorporation of nuclear quantum mechanical effects into simulations of chemical reactions in solution and in enzymes is a challenging task because it is necessary to average over protein conformations and solvent configurations.[1−3] These effects, including zero-point energy and tunneling, are particularly significant for proton and hydride transfer reactions, which are ubiquitous in chemical and enzymatic processes.[1] A widely used approach to probe quantum mechanical tunneling is through measurements of primary and secondary kinetic isotope effects.[4] For example, in two of the most extensively studied enzyme reactions,[5−8] the hydride transfer reaction by liver alcohol dehydrogenase[5,6,9,10] and the proton-transfer reaction by methylamine dehydrogenase[7,8,11] have been shown to have significant tunneling contributions. Both experimental and computational studies suggest that tunneling makes little contributions to *catalysis*,[2] which is related to the rate enhancement by an enzyme relative to the uncatalyzed process in water. It is, nevertheless, essential to include quantum mechanical effects to determine kinetic isotope effects and to estimate the reaction rates quantitatively.[1,3,12] Furthermore, a number of theoretical studies have shown that the inclusion of zero point energy can reduce free energy barriers by 2−3 kcal/mol for enzyme reactions.[10,13,14]

Several simulation methods have been used to determine kinetic isotope effects in enzymatic reactions, including the ensemble-averaged variational transition state theory with multidimensional tunneling (EA-VTST),[9] discretized path integral simulations,[15−17] and a multiconfiguration wave function method.[10] These methods have been applied to several enzymatic reactions with good accord between the calculated and experimental kinetic isotope effects.[1] The EA-VTST approach also has the advantage of separating contributions from bound vibrations and tunneling, providing further insights into the reaction mechanism. In this paper,

* Corresponding author e-mail: gao@chem.umn.edu.

† Present address: Institute of Biotechnology and Biomedicine, Universitat Autònoma de Barcelona, Bellaterra 08193, Catalunya, Spain.

10.1021/ct050257t CCC: $33.50
Published on Web 01/26/2006

we describe the implementation of a bisection sampling algorithm in centroid path integral simulations and examine the convergence properties in these calculations for two proton-transfer reactions in solution;[18−20] the first system is a model reaction of $[H_3N-H-NH_3]^+$ and the other is the proton abstraction of nitroethane by acetate ion, modeled for the enzymatic process in nitroalkane oxidase. We implement an approach similar to that described by Hwang et al.[15,16] and by Sprik et al.,[21] in which the quantum mechanical effects are incorporated into the rate calculation through a transmission coefficient by correcting the classical potential of mean force (PMF) obtained from Monte Carlo or molecular dynamics simulations.[2,3,22] Thus

$$k^{qm} = \gamma k^{TST} \tag{1}$$

where k^{qm} is the quantum mechanical rate constant and k^{TST} is the classical transition state theory (TST) rate constant. In general, the transmission coefficient in eq 1 is a product of the deviation from equilibrium behavior, the classical dynamic recrossing factor, Γ, and the quantum mechanical correction, κ.[2,3] Here, we focus on the quantum mechanical contributions, which are defined as follows[15,16]

$$\kappa = e^{-\beta(G^{\ddagger}_{qm} - G^{\ddagger}_{TST})} \tag{2}$$

where $\beta = 1/k_B T$, k_B is Boltzmann's constant, T is the temperature, and $G^{\ddagger}_{qm}$ and $G^{\ddagger}_{TST}$ are the quantum and classical free energy of activation, respectively.

Although the quantum mechanical free energy of activation, $G^{\ddagger}_{qm}$, can be obtained directly by using centroid path integral molecular dynamics simulations,[23−27] Hwang et al. noted that it is more convenient to evaluate the free energy difference, $G^{\ddagger}_{qm} - G^{\ddagger}_{TST}$, in eq 2.[15,16] Thus, rather than carrying out a full centroid path integral simulation directly, one performs classical molecular dynamics simulations to obtain the potential of mean force along a reaction coordinate, and then a quantum correction is made along the classical reaction path.[15,28] This provides a quantum correction to the classical results. A similar idea was originally described by Sprik et al.,[21] who proposed a procedure to obtain quantum mechanical averages through free-particle path integral sampling over classical configurations from molecular dynamics or Monte Carlo simulations.

$$\langle A \rangle = \langle \langle A \rangle_K^{FP} \rangle_{CM} \tag{3}$$

In eq 3, the inner average $\langle A \rangle_K^{FP}$ represents the quantum average of property A by path integral sampling of free-particles over a fixed configuration K, in which the center of mass (centroid) positions are constrained to those of the classical particle positions. The outer average is over "classical" configurations. This double averaging strategy is the essence of the quantized classical path (QCP) method exploited by Hwang et al.,[15] which employs the trajectory obtained from classical molecular dynamics simulations to obtain the QM correction by performing free-particle path integral averaging. The QCP method can be used to treat nuclear QM effects in macromolecular systems, and it has been applied to several enzymatic reactions.[15,17,29,30]

A central issue in path integral simulations is convergence. It appears that a direct sampling procedure was used in previous QCP applications to enzymatic reactions. Åqvist and co-workers used the QCP approach to calculate the kinetic isotope effect in the proton-transfer reaction catalyzed by glyoxalase I.[17] In this study, 20 particle-beads were used to describe the quantized paths, and for each classical configuration, 1, 5, and 10 Monte Carlo Metropolis steps were used, respectively, to obtain the quantum corrections. In another calculation, a total of 20 000 free-particle configurations were used for 18 beads along the entire reaction coordinate for an enzymatic reaction.[30] Other studies indicate that more extensive path integral sampling might be needed even for a dilute hard-sphere system.[21] In the present study, we use a bisection free-particle sampling method,[19] coupled with the QCP approach to enhance convergence.[15] The convergence properties of the method are scrutinized with a view to arrive at a practical scheme for condensed phase simulations. Here, we present results for the two model proton-transfer reactions in aqueous solution mentioned above. The first reaction is the symmetric proton transfer between an ammonium ion and an ammonia molecule (reaction I). The second reaction is between nitroethane and an acetate ion (reaction II)

$$NH_4^+ + NH_3 \rightarrow NH_3 + NH_4^+$$

$$CH_3CO_2^- + CH_3CH_2NO_2 \rightarrow CH_3CO_2H + CH_3\bar{C}HNO_2$$

The convergence of the QM correction to the classical PMF is analyzed with respect to the sampling of the path-integrals, the solution phase classical configurations, and the number of ring polymer beads. The conclusions from the current work will be useful in future simulations of solution phase and enzymatic reactions.

Theoretical Background

The centroid quantum mechanical partition function for a ring of P quasi-particles or beads in the discrete path integral form is given as follows[31]

$$Q_P^{qm} = \int d\bar{\mathbf{x}} \left(\frac{1}{4\pi\Lambda^2}\right)^{P/2} \int dx_1 \cdots \int dx_P e^{-\beta V^{qm}} \tag{4}$$

where $\beta = 1/k_B T$, P is the number of quasi-particles of the discrete path, and the average or centroid position, $\bar{\mathbf{x}}$, of the quasi-particle positions, $\{x_i; i = 1, \cdots P\}$, is defined as

$$\bar{\mathbf{x}} = \frac{1}{P}\sum_{i=1}^{P} x_i \tag{5}$$

In eq 4, the effective potential $V^{qm}(x_1, \cdots, x_p)$ is given by

$$V^{qm}(x_1, \cdots, x_p) = \frac{1}{4\beta\Lambda^2}\sum_{k}^{P}(x_k - x_{k+1})^2 + \frac{1}{P}\sum_{k}^{P} U(x_k) \tag{6}$$

and Λ is the thermal de Broglie wavelength

$$\Lambda = \left(\frac{\beta\hbar^2}{2mP}\right)^{1/2} \tag{7}$$

where m is the mass of the particle. Thus, each quasiparticle is connected by a harmonic spring with its two neighbors and is subjected only to a fraction, $1/P$, of the full classical potential, $U(x_i)$. The discrete paths are circular with $x_{P+1} = x_1$. The exact QM partition function is obtained in the limit

$$Q^{\mathrm{qm}} = \lim_{P\to\infty} Q_P^{\mathrm{qm}} \tag{8}$$

In the quantized classical path (QCP) approach,[15] Warshel and co-workers showed that the QM correction to classical free energy along a reaction path can be determined by a double average of classical and free-particle path integral simulations, making use of the assumption that the centroid positions coincide with the classical coordinates.[24,32] Thus

$$G^{\ddagger}_{\mathrm{qm}}(\bar{x}) - G^{\ddagger}_{\mathrm{TST}}(\bar{x}) = -\frac{1}{\beta}\ln\frac{Q_P^{\mathrm{qm}}}{Q_P^{\mathrm{cm}}} = -\frac{1}{\beta}\ln \ll e^{-\beta/P\sum_k^P \Delta U_k} >_{\mathrm{FP},\bar{x}} >_{U(\bar{x})} \tag{9}$$

where Q_P^{cm} is the reference classical (CM) partition function, and $\Delta U_k = U(x_k) - U(\bar{x})$. Here, the outer average $< \cdots >_{U(\bar{x})}$ is obtained according to the distribution generated by propagating classical molecular dynamics or Monte Carlo simulations using the potential $U(\bar{x})$. The inner average $< \cdots >_{\mathrm{FP},\bar{x}}$ is over the free particle distribution, in the absence of any external potential[15]

$$< e^{-\beta/P\sum_k^P \Delta U(x_k)} >_{\mathrm{FP},\bar{x}} = \frac{\int \delta(\bar{x}) e^{-\beta/P\sum_k^P \Delta U(x_k)} e^{-1/4\beta\Lambda^2\sum_k^P (x_k - x_{k+1})^2} dx_1 \cdots dx_P}{\int \delta(\bar{x}) e^{-1/4\beta\Lambda^2\sum_k^P (x_k - x_{k+1})^2} dx_1 \cdots dx_P} \tag{10}$$

where the integration of beads is constrained at the centroid position $\bar{\mathbf{x}}$. The advantage of this formulation is that one can sample the free particle (FP) distribution (i.e. the quasiparticle polymer rings) separately at each CM configuration (i.e. centroid position) and then average over all CM configurations obtained from molecular dynamics simulations.

Computational Details

A. Convergence. Although eqs 9 and 10 provide a very appealing framework for obtaining quantum averages by carrying out classical simulations on a classical potential $U(\bar{x})$, a main practical problem is that most configurations obtained from the free-particle sampling procedure (inner average of eq 9) have very small contributions to the total average in the external potential $U(\bar{x})$. Only a tiny fraction of the free particle configurations have sufficiently large probabilities in the actual physical environment. Thus, unless an efficient free particle sampling procedure is used, it would be very difficult to achieve convergence using eq 10.

In principle, it is possible to find a subset of free particle configurations that carry the greatest weight to the path integral average in QCP calculations. However, for a given potential energy surface, these free particle configurations are generally not known, unless the potential energy surface and Hessian for each classical configuration have been enumerated.[27] Therefore, it is necessary to comprehensively sample the free particle distribution. Moreover, to ensure convergence from PI calculations, it is necessary to increase the number of beads until the desired property is converged. We have often encountered diverging averages in the quantized classical path approach as the number of particle beads is increased if a direct sampling procedure is used for the free particle distributions. This is because the spring connecting the polymer beads becomes increasingly stiff as the number of beads increases, which makes it more difficult to sample. In fact, the equilibration time of the slowest mode in the ring polymer scales as $(P/\pi)^2$ where P is the number of beads.[19,20] It has been noted that standard Metropolis Monte Carlo and molecular dynamics simulations are not the optimal choice as a free particle sampling algorithm.[33]

In the present study, we employed the bisection scheme introduced by Ceperley and co-workers,[19,20] which turns out to be the most effective method in our application. Here, the free-particle distribution can be sampled exactly because it is a Gaussian of known mean and width

$$\rho(x_i, x_m; \beta/P) = \left(\frac{1}{4\pi\sigma}\right)^{1/2} e^{(x_i - x_m)^2/2\sigma} \tag{11}$$

where the variant of the Gaussian is the square of the de Broglie wavelength $\sigma = \Lambda^2$, and

$$x_m = \frac{(x_{i-1} + x_{i+1})}{2} \tag{12}$$

We have implemented the bisecting method proposed by Ceperley in QCP calculations,[19] which is a combination of multilevel Monte Carlo[20] and the Lévy construction for sampling a free particle path.[34] The bisection method takes advantage of the fact that the density matrix at a given temperature may be written as the integral of two density matrices at a higher temperature.[19] Thus one can accurately sample the free-particle distribution at a higher temperature and more effectively explore the configurational space. The present bisection quantized classical path sampling is called BQCP.[18]

Specifically, for each free particle move, we select a random sequence of N-1 consecutive beads in the polymer ring, where $N = 2^l$ and l is called the level of bisection.[19] The ends of the bead sequence are fixed at r_i and r_{i+N}. In principle, the two endpoints could be the same bead, when the entire polymer ring is sampled at each step, which will generate entirely uncorrelated configurations. At the coarsest level of bisection, $k = l$, the position of the bead in the midpoint of the sequence is first sampled, which is placed at the geometrical center of the two end points and randomly displaced according to the Gaussian distribution of width $2^{l-1}\sigma$, $r_{i+N/2} = (r_i + r_{i+N})/2 + \xi$, where ξ is the random displacement vector. Having sampled the $r_{i+N/2}$ point, we bisect the two new intervals, $(r_i, r_{i+N/2})$ and $(r_{i+N/2}, r_{i+N})$ at the next bisection level $k = l - 1$ with the distribution width $2^{l-2}\sigma$, to sample points at $r_{i+N/4}$ and $r_{i+3N/4}$. This bisecting procedure continues recursively until level $k = 1$, where all $N-1$ beads have been sampled. As in the single bead sampling, the acceptance ratio for such a "Monte Carlo"

Table 1. Reaction and Transition State[a] Energies for Reactions I and II

	AM1	AM1-SRP	ab initio
reaction I	0.0 (3.3)	ND	0.0 (2.6)[b]
reaction II	−9.6 (3.1)	7.5 (11.7)	9.8[c](12.5)[d]

[a] Transition state energies in parentheses. [b] Reference 51. [c] Reference 45. [d] MP2/6-31+G(d)// MP2/6-31+G(d).

move will be 100% since the new positions are drawn from the accurate free-particle distribution.[19] After each move, the polymer ring is recentered at the classical position to enforce the centroid constraint. In our implementation, the Box-Muller transformation is used to generate the random displacements with a Gaussian distribution.[35]

The BQCP method has been implemented in the CHARMM simulation package[36] in version c32a2 in a serial and a parallel version. The quantum correction to the classical PMF curves were fitted to an inverse Eckart potential using the Levenberg−Marquardt nonlinear optimization method.[35] The QM correction along the reaction coordinate is assumed to be a smooth, continuous function.[18]

B. Potential Energy Function. To describe nuclear quantum effects in aqueous phase reactions, it is essential to employ a potential energy function that can describe the bond breaking and formation process. We adopted a strategy that combines a quantum mechanical model with a molecular mechanical force field, or combined QM/MM potential, in molecular dynamics simulations. Thus, the solute molecules are treated by quantum mechanics, and the solvent is represented by the three-point charge TIP3P model for water.[37] The total energy of the system is

$$E_T = E_{QM} + E_{QM/MM} + E_{MM} \tag{13}$$

where E_{QM} is the solute energy, E_{MM} is the solvent energy, while $E_{QM/MM}$ is the energy term for interactions between QM and MM atoms. Combined QM/MM methods have been used to study a variety of chemical reactions in the gas-phase, and in condensed phases, including enzymes, and have been described in a number of review articles.[38−42]

In the proton transfer between two ammonia molecules the standard AM1 semiempirical Hamiltonian was employed, as it has been shown to give reliable results for this system (Table 1). However, for the nitroethane-acetate reaction, neither the AM1 nor the PM3 method yielded satisfactory energetic results in comparison with ab initio data at the G3 level. Thus, we developed a set of reaction specific parameters (AM1-SRP), using AM1 as a starting point for a full nonlinear optimization of the parameter space.[43] The parametrization was performed in a stepwise manner, at each step allowing additional parameters to be optimized simultaneously. The process commenced with the U_{ss}, U_{pp}, β_s, and β_p parameters allowing changes up to 15% from the original AM1 values. At the second step the ζ_s, ζ_p, and α parameters were also allowed to change up to 10%, while the subsequent step allowed the Gaussian terms L and M to change up to 5%, followed by the K Gaussian terms, which were also allowed to change by the same amount. At the final level of optimization, the 2 electron terms G_{ss}, G_{sp}, G_{pp}, G_{p2}, and H_{sp} were allowed to change up to 2.5%. Thereafter, the parameters were further optimized to fine-tune the fit to the target data. Only gas-phase molecular descriptors for the reactant and product states were employed as target data in the parametrization process. The descriptors used were molecular heats of formation available for three of the four reactant/product species (acetic acid, acetate, and nitroethane). The remaining heat of formation (nitroethyl anion) was obtained from the three other heats of formation and the computed G3 reaction energy. Additionally, MP2/6-31+G(d) bond distances and angles as well as selected frequencies were used as target data. To allow for an accurate description of the charge distribution in the molecules, Mülliken charges and dipole moments (for the neutral species) computed at the MP4/6-31+G(d) level were used as target data; however, the charge restraint was used primarily to ensure balanced charge polarization rather than strictly fitting these charges. Such a careful parametrization protocol yields an inexpensive, yet highly accurate Hamiltonian that is suitable for QM/MM simulations. The final AM1-SRP yielded a reaction energy of 8.0 kcal/mol in good agreement with the G3 value of 9.8 kcal/mol (Table 1),[44] and these parameters have been given in ref 45.

C. Simulation Details. The solutes were embedded in cubic boxes of water molecules. In the case of reaction I the size of the box was 25 Å^3 giving a total of 502 water molecules. In reaction II, the system dimensions were ∼30 Å^3, resulting in 898 water molecules. Internal water bond distances were constrained to the experimental value using the SHAKE algorithm in all simulations.

In reaction I a spherical group based cutoff of 14 Å was used for both van der Waals and electrostatic interactions. However, for reaction II we employed the particle-mesh Ewald summation method for QM/MM simulations[46] to obtain high-accuracy results enabling direct comparison with experimental data. In these simulations, the van der Waals cutoff was group-based and set to 9.5 Å. All simulations employed molecular dynamics propagated using the leapfrog Verlet algorithm with a 1 fs time step.[47] Periodic boundary conditions were used together with the canonical ensemble (NVT) for reaction I and the isobaric−isothermal ensemble (NPT) for reaction II, both at 25 °C. For each simulation (or window, see below), 100 ps of equilibration was first carried out, which was followed by averaging for 100 ps.

The potential of mean force (PMF) profiles were obtained using the umbrella sampling technique.[48,49] According to this approach the reaction is divided into a series of windows, and in each window a biasing potential (umbrella potential) is applied to allow the reaction to climb over the barrier within the time frame of molecular dynamics simulations. The effect of the biasing potential is subsequently removed when the separate windows are combined to produce the PMF profile. This was done using the weighted histogram analysis method.[50] In the current simulations, between 7 and 15 windows were used to span the reaction coordinates for reactions I and II. The reaction coordinates were defined as the difference between the breaking and forming bonds.

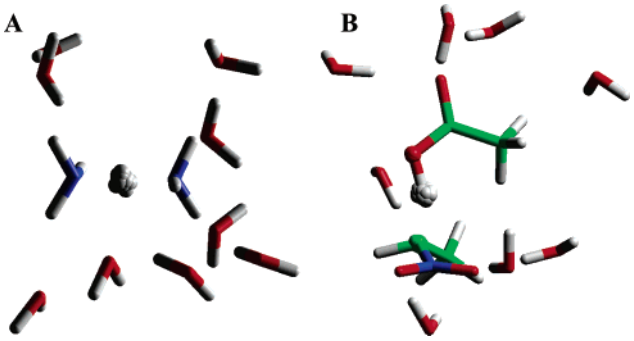

Figure 1. Snapshots of instantaneous structures from combined QM/MM molecular dynamics and quantized classical path simulations for (A) the proton transfer in $NH_4^+ + NH_3$ and (B) the deprotonation of nitroethane by an acetate ion in aqueous solution.

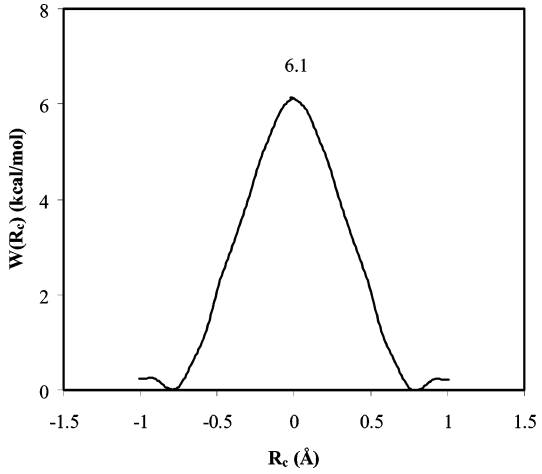

Figure 2. Classical potential of mean force for the NH_4^+-NH_3 proton-transfer reaction in aqueous solution.

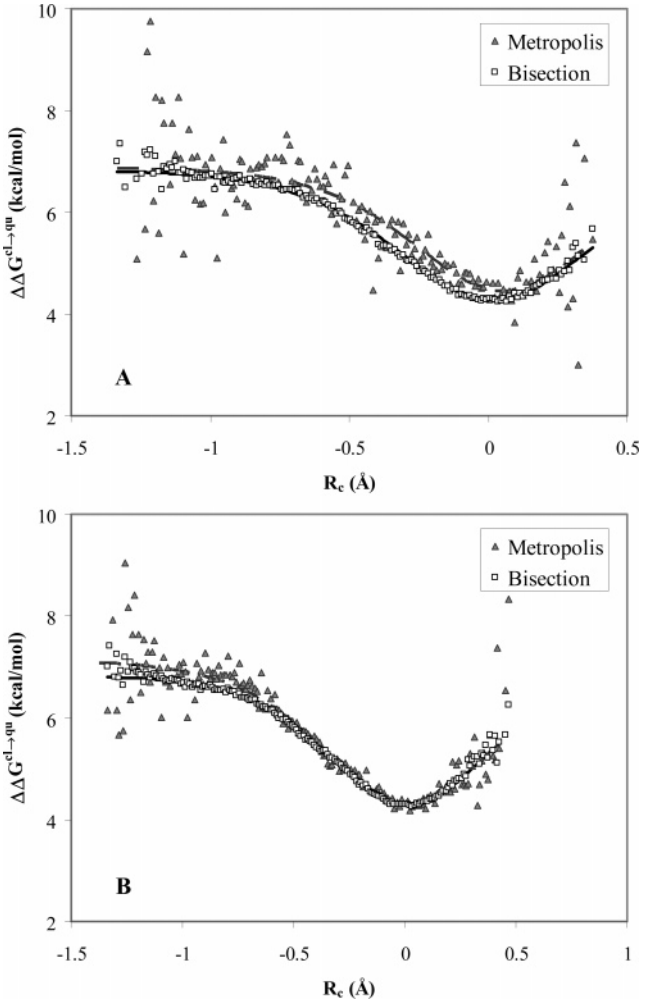

Figure 3. Comparison of the nuclear QM correction for the NH_4^+-NH_3 proton-transfer reaction in aqueous solution using the QCP method with the Metropolis and Bisection sampling schemes.

Results and Discussions

A. Proton Transfer between NH_4^+ and NH_3. The computed classical free energy barrier for reaction I (Figure 1A) is in reasonable agreement with previous results of Garcia-Viloca et al.,[13] although the currently computed barrier of 6.13 kcal/mol (Figure 2) is lower than in that work (11 kcal/mol). The reason for the difference is the use of a fixed nitrogen distance of 3 Å in the previous study,[13] whereas this geometrical parameter was not constrained in the present simulations. This view is supported by two-dimensional PMF simulations performed for this reaction, which showed that the optimal heavy atom distance for proton transfer is ca. 2.6 Å.[51]

We estimated the quantum correction to the classical reaction profile for the proton transfer reaction using the classical trajectories that were saved every 100 integration steps. Initially it is of interest to compare the performance of the QCP method between the standard Metropolis sampling and the bisection sampling of free particles. The use of standard Metropolis sampling with QCP for enzymatic systems has been shown to yield excellent results even with a small number of configurations.[17] However, we were unable to obtain converged results with standard Metropolis sampling of the free particles.[19] Nevertheless, we found that the QCP method coupled with the bisection algorithm converges quickly and obtained reasonable results for model systems.[18] Thus, a systematic comparison between the different sampling schemes for a chemical reaction in the condensed phase is presented. The result of such a comparison of the two sampling methods for reaction I is shown in Figure 3. This test case used 16 beads for each of the three atoms directly involved in the proton transfer (N−H- - -N), similar to the number of beads used in related PI studies.[17] A total of 7000 classical configurations (corresponding to 1000 sets of coordinates from each of the 7 windows used in the classical umbrella sampling simulations, spanning 700 ps) saved at 0.1 ps intervals were used, and each classical point was subjected to 100 MC steps of free particle path integral sampling. This scheme is denoted by (7K/100). It is evident from the results that the use of an accurate free particle distribution greatly improves the convergence of the QM correction to the classical potential energy surface. Using the bisection sampling scheme, a QM correction of 2.53 kcal/mol is obtained. Note that we use two decimal digits in the discussion purely for the purpose of comparing convergence as the overall statistical errors in the computed potential of mean force are about 0.5 kcal/mol based on experience from umbrella sampling simulations starting from different initial

configurations and conditions. The reaction coordinate position of the maximum QM barrier correction is located at 0.01 Å, close to the expected value of zero for a symmetric reaction and is within the statistical accuracy of the data averaging. The convergence of the bisection results was tested by increasing the number of classical steps to 35 000 (35K/100). The results were found to be within ±0.005 kcal/mol, and the position of the maximum QM barrier correction is located at 0.01 Å (Figure 3B). Using the direct Metropolis procedure with a 7K/100 sampling scheme, a QM correction of 2.41 kcal/mol is obtained, with a maximum correction located at 0.05 Å (Figure 3A). Considering that the polymer chains were equilibrated for 1 000 000 steps prior to data collection, we attribute the small difference to incomplete convergence. This conclusion is corroborated by inspecting the χ^2 values obtained from the nonlinear fitting of an inverse Eckart potential to the QM correction curves. Using the bisection sampling scheme, a χ^2 value of 26 is obtained, while with Metropolis sampling χ^2 is 1198. After increasing the number of classical steps to 35000 (35K/100), the QM correction was found to be 2.77 kcal/mol, and the position of the maximum QM barrier correction is located at 0.02 Å. Thus, the results have not yet converged, and additional Metropolis sampling of the PI would be necessary to obtain converged results.

To further probe the convergence behavior of the BQCP method with respect to the number of quantized atoms and the extent of sampling, additional tests were performed for reaction I. These tests used 32 beads, as this has been found to be a reasonable compromise between computational cost and accuracy.[18] The results for three levels of quantization are shown in Figure 4, where 7000 classical configurations were used in conjunction with 100 path integral steps per classical configuration (7K/100). At the lowest level of quantization, only the transferring hydrogen is treated as a ring polymer, while the remaining atoms are classical entities. At the second level, the three transferring atoms are treated quantum mechanically. At the final level, all solute atoms are treated by PI simulations. The quantum mechanical correction obtained when quantizing the transferring proton only is 2.72 kcal/mol, and when quantizing the donor and acceptor heteroatoms as well, the correction term is very similar at 2.67 kcal/mol. Quantizing all solute atoms introduces considerable challenge, due to the large number of hydrogens, which have long de Broglie wavelength and are therefore more difficult to sample. For this particular system, convergence is difficult to achieve when all solute atoms are quantized. With the 7K/100 scheme, a QM correction of 2.81 kcal/mol is obtained. With additional sampling of the classical configuration, using a 14K/100 sampling scheme, the QM correction is 2.59 kcal/mol. It seems that the free particle distribution has not yet been sufficiently sampled, and it is necessary to perform more extensive path integral sampling or to add additional classical configurations.

For reaction I, quantization of only the transferring atom is sufficient to yield reliable results. It is clear from the results that as the number of quantized particles increases, so does the complexity of the ring polymer configurational space.

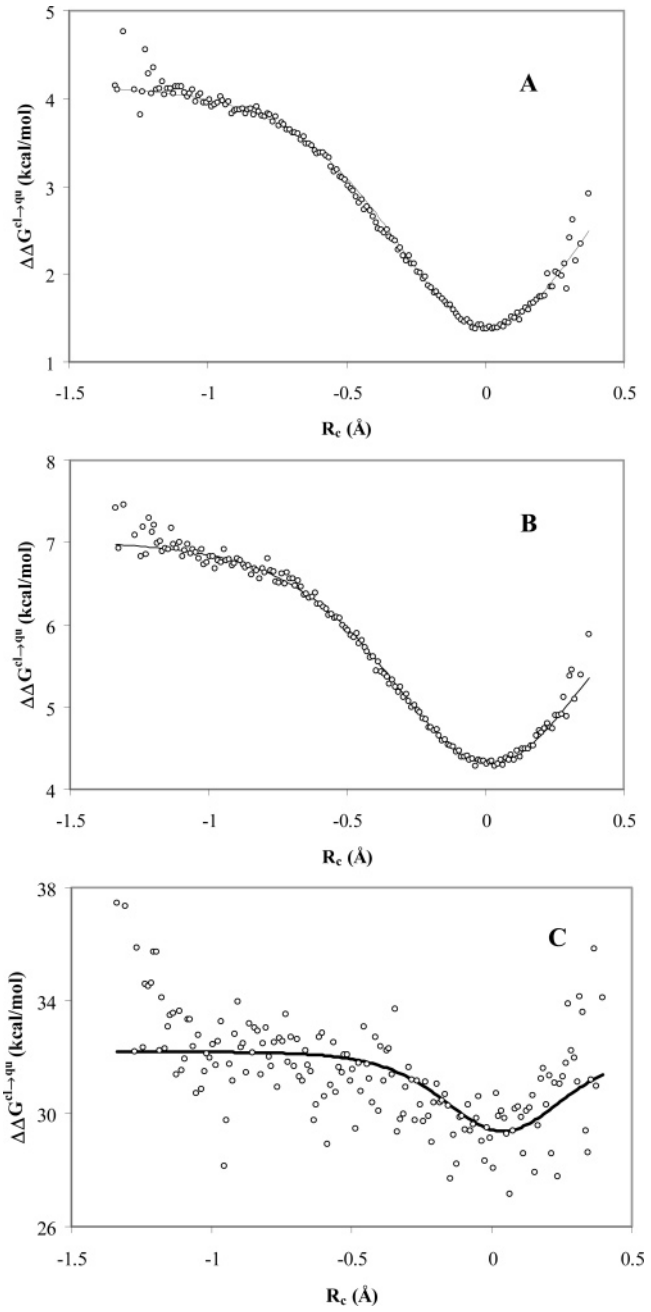

Figure 4. Comparison of the BQCP correction for the NH_4^+-NH_3 proton-transfer reaction in aqueous solution at different levels of quantization: (A) the transferring proton only, (B) the transferring proton plus the donor and acceptor nitrogen atoms (N−H- - -N), and (C) the entire solute (NH_4^+-NH_3).

Thus, quantizing a single atom yields rapid convergence while extending the nuclear QM region slows down the convergence. In a thorough investigation, Tuckerman and Marx showed that the quantum nature of the heavy atoms can substantially enhance proton tunneling by as much as 31% compared to a classical frame in the case of malonaldehyde.[52] Similar findings have also been noted by Hinsen and Roux on acetylacetone.[53] To complement previous convergence tests for simple model systems,[18] we also tested several different sampling schemes to arrive at one that yields the optimal compromise between accuracy and computational cost. In all of the following test cases, the three central atoms

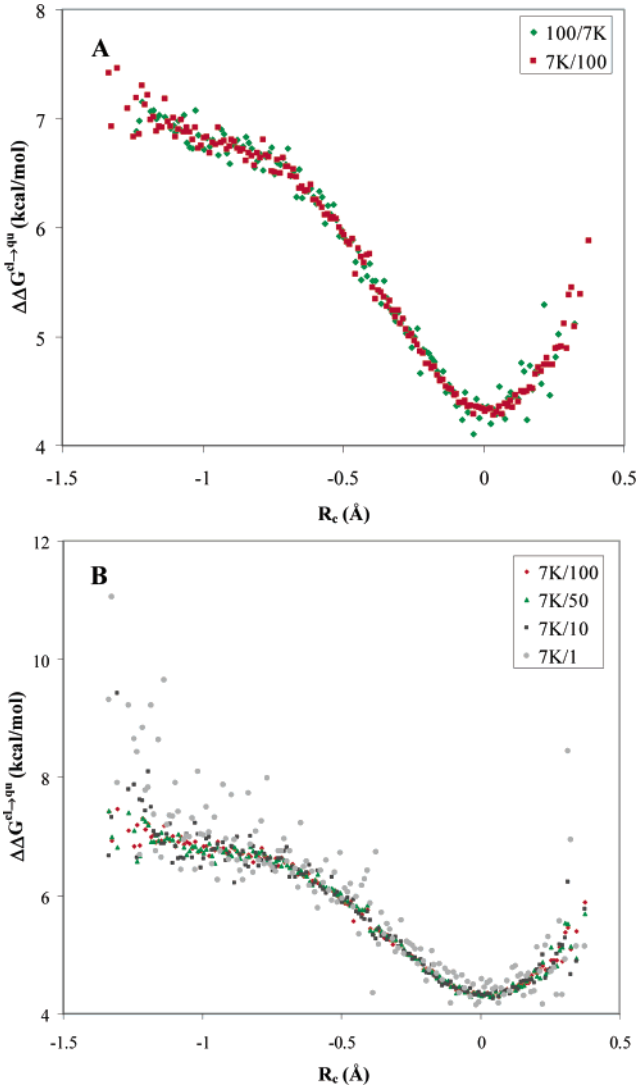

Figure 5. Comparison of different BQCP sampling schemes for the NH_4^+-NH_3 proton-transfer reaction in aqueous solution.

directly involved in the proton transfer were quantized using 32 beads unless otherwise stated.

Previous studies have shown that for a simple Morse potential, approximately 1000 classical configurations coupled with 100 PI steps per classical (centroid) configuration, yields good convergence.[18] Thus, we used this conclusion as a starting point in the present test. In Figure 5A, two sampling schemes, requiring comparable computational cost, are compared. In the first scheme, 7000 classical configurations are coupled with 100 path-integral sampling steps. The second scheme uses 700 classical configurations and 1000 PI steps. Fitting of an inverse Eckart potential to the curves reveals identical QM corrections of 2.67 kcal/mol. However, from the distribution of the points it is clear that a scheme that samples the classical configuration space more extensively is preferable to additional sampling of the polymer rings at each centroid position. This is due to the greater variance in the free particle path-integral estimator (eq 10) than in the external average over the free-particle paths (eq 9).

In Figure 5B, additional such sampling schemes are presented, using 7000 classical configurations, and 100, 50, 10, and 1 PI steps. Although the results indicate that it would be preferable to use 100 PI steps per classical configuration, using 50 or even 10 yields reasonable results. The QM corrections obtained by sampling 100, 50, 10, and 1 quasi-particle configuration(s) at each classical step are 2.67, 2.64, 2.63, and 2.71 kcal/mol, respectively (Figure 5B). The position of the maximum QM correction is 0.01 Å for the former three, whereas for the latter the location has shifted to 0.02 Å.

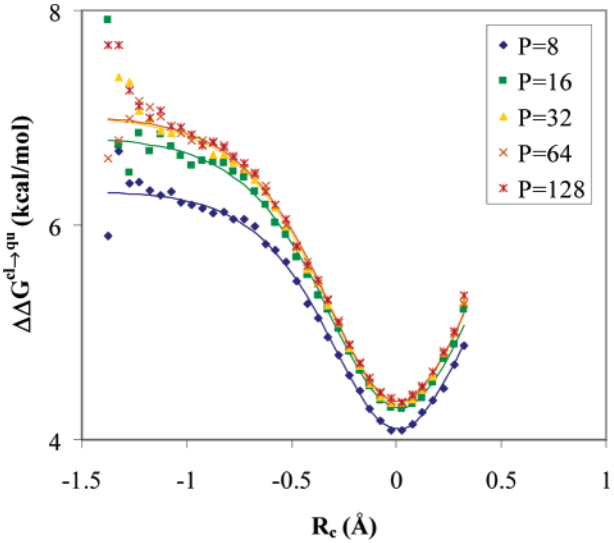

Figure 6. BQCP correction for the NH_4^+-NH_3 proton-transfer reaction in aqueous solution at different levels of path-integral discretization.

The extent of ring polymer beads required to obtain converged QM corrections was also investigated. Due to the great cost of PI simulations with a large number of beads, in the following test cases we used a scheme of 35 000 classical steps, each of which consists of 10 PI sampling steps. The results presented in Figure 6 show that the QM corrections to the computed classical free energy barrier increases with increasing number of beads. At the lowest level of discrete path description, using only 8 beads, we obtained a QM correction of 2.21 kcal/mol. Increasing the number to 16 improves the results at 2.50 kcal/mol, and 32 beads give a value of 2.64 at double the cost. Employing 64 beads yields identical quantization energy at 2.64 kcal/mol. A QM correction of 2.66 kcal/mol is obtained when doubling the number of beads to 128, thus indicating that a reasonable converged value is achieved with 32 beads. Thus, as was observed in our previous studies, using 32 beads seems to be a reasonable compromise between accuracy and cost.

A direct comparison of the results obtained herein with the results of Garcia-Viloca et al.[13] is not feasible due to the different methods employed. In the previous work only quantized vibrations were accounted for, while the current BQCP simulations account for both quantized vibrations and tunneling. In the work of Garcia-Viloca et al.,[13] a quantum correction of 2.0 kcal/mol was obtained, although the contribution of the mode corresponding to the reaction coordinate was not reported in that work. Thus, we performed instantaneous normal-mode analysis of the trajectories from the current simulations as well as tunneling calculations

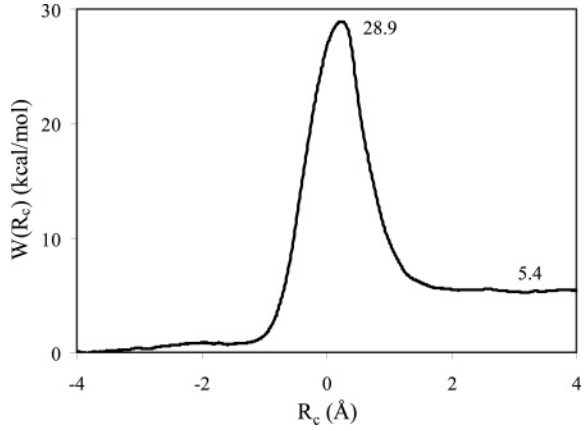

Figure 7. Classical potential of mean force for the deprotonation of nitroethane by an acetate ion in aqueous solution.

within the ensemble-averaged variational transition-state theory with multidimensional tunneling (EA-VTST/MT) approximation. The vibrational contribution to the quantized free energy amounts to 2.4 kcal/mol, in reasonable accord with ref 13 considering the small difference in the definition of the reaction coordinate. Tunneling does not seem to play a major role in the present system. The absence of tunneling is somewhat surprising considering the study of Truhlar et al.,[54] where tunneling was found to play a role in increasing the reaction rate. A reason for this difference may be the PM3 Hamiltonian used in that study, as opposed to AM1 which was utilized here. Indeed, the PM3 reaction barrier in solution was found to be in the range 13.3−15.9 kcal/mol,[54] compared to 6.1 kcal/mol obtained here with AM1.

B. Deprotonation of Nitroethane by Acetate Ion. The second reaction investigated is the ionization of nitroethane by an acetate ion in water (Figure 1B). This reaction is of particular interest because it is an analogue of the ionization of nitroethane by nitroalkane oxidase (NAO).[55−57] In this reaction, the active site residue Asp402 is the nucleophile that abstracts the α-proton of small nitroalkane substrates.[57] Moreover, the experimental reaction rate and kinetic isotope effects at several temperatures are available for this reaction.[55] The classical PMF yields a barrier of 28.90 kcal/mol (Figure 7), placing it slightly above the experimentally observed value of 24.8 kcal/mol.[55] Addition of nuclear quantum effects, which are dominated by the zero-point energy, lowers this classical value, as discussed below.

In the present test, a crucial question is the number of atoms to be quantized in the centroid PI simulation. In light of the conclusions obtained for reaction I, the BQCP simulations for reaction II used 32 beads and 10 PI steps per classical step, unless otherwise stated. The classical trajectories were saved every 25 steps.

Initially, only the transferring proton was quantized, yielding a QM correction value of 2.75 kcal/mol and a combined reaction barrier of 26.15 kcal/mol. A total of 27 000 classical configurations from 10 windows of umbrella sampling calculations were used to obtain the results. Comparison of results using different number of classical (centroid) configurations indicates that the results have converged. At the next level of quantization, we treated the three core transferring solute atoms as ring polymers. This allows for additional quantum effects to be included. We obtained a quantum correction of 3.03 kcal/mol, giving a reaction barrier of 25.87 kcal/mol in agreement with experiment.[45,55] A total of 38 000 classical steps were used to obtain the results. To better account for multidimensional nuclear QM effects, we additionally quantized the three neighboring heavy atoms (bonded to the transferring atoms). To obtain converged results, a total of 45 000 classical structures were employed, spanning 1.1 ns of MD simulations. Thus, we obtained a QM correction of 3.11 kcal/mol, placing the computed barrier of 25.79 kcal/mol in agreement with the experimental value. Although the difference is rather small, there is a gradual increase in the quantum correction as the number of quantized particle increases. Thus, to account for the QM correction to the barrier height of a classical PMF, it is important to include the donor and acceptor atoms in addition to the transferring light atom. This is in contrast to the ammonium ion-ammonia reaction where it seems to be sufficient only to quantize the transferring light particle. This difference is due to the greater rehybridization involved in the nitroethane-acetate ion reaction. Additionally, including the neighboring atoms has a small but noticeable effect on the QM correction to the barrier. However, inclusion of additional atoms impedes on the convergence of the free particle PI sampling, thus requiring additional sampling. The dependence of the QM correction on the number of classical configurations is illustrated in Figure 8 for the largest QM system. With a bin size of 0.001 Å, corresponding to ca. 20 configurations per bin, $\Delta\Delta G^{cl\rightarrow qu}$ fluctuates greatly. However, as the bin size increases, and thereby also the number of configurations per bin, the variance within each bin is reduced. When increasing the bin size from 0.05 to 0.1 Å no considerable change in $\Delta\Delta G^{cl\rightarrow qu}$ is observed, indicating that convergence with respect to classical configurations has been reached.

To verify that the use of 32 beads is reasonable for the current system, we also experimented with 16, 64, and 128 beads per quantized particle. To this end, we chose a quantized subsystem consisting of the transferring proton and the donor and acceptor atoms. Using 16 beads the QM correction was estimated as 2.86 kcal/mol, somewhat below the value obtained with 32 beads (3.03 kcal/mol). Increasing the number to 64 and 128 beads both yield a slightly larger value of 3.06 kcal/mol. Thus, employing 32 beads seems a reasonable choice in the case of reaction II as well.

Additionally, the second Cα hydrogen was added to the PI atom list, and although this increased the absolute QM correction value, it had a small effect on the barrier height.

To further test the BQCP method, we also studied the convergence of the computed KIE. In particular, we tested the importance of the number of quantized solute atoms, in obtaining reliable computed KIE. Quantizing only the transferring proton, the computed QM correction difference between proton and deuteron transfer is 1.06 kcal/mol, with a minimum in the QM correction curve at 0.1 Å. When combined with the classical PMF, this yields a computed KIE of 5.4 for a singly deuterated nitroethane. The total KIE is increased to 6.0 when secondary effects (1.10) are accounted for.[45] This may be compared to the experimental

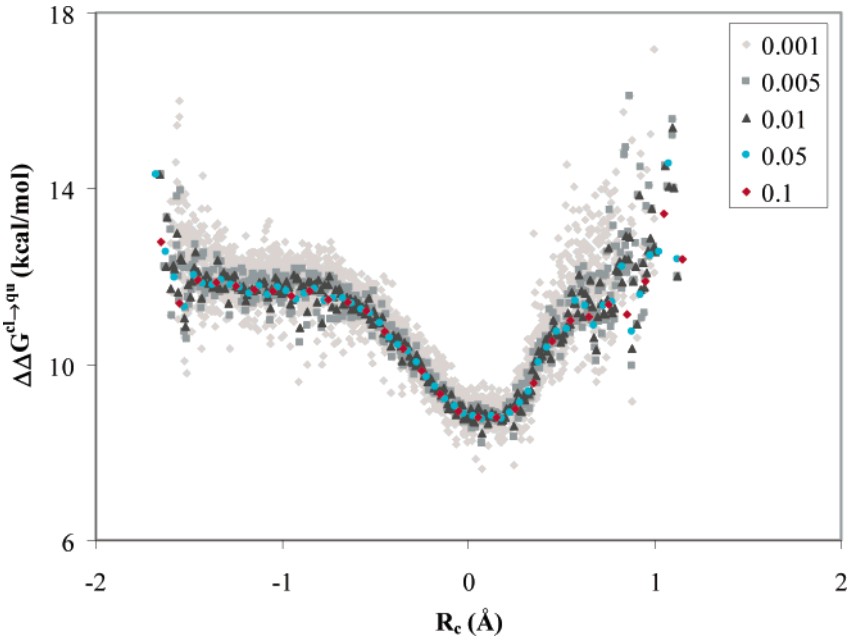

Figure 8. Computed average quantum corrections to the classical potential of mean force for the deprotonation of nitroethane by an acetate ion in aqueous solution, determined using different bin sizes in the quantized classical path averaging. Smaller bin sizes give relatively larger fluctuations, whereas a large bin width yields smooth results along the reaction path.

value of 7.8.[55] In free energy terms, the difference is about 0.1 kcal/mol. Increasing the number of beads to 64 and 128 did not narrow the difference between the experimental and the computed KIE (results not shown). Using 16 beads resulted in a considerable lower KIE of 4.3. Quantizing the donor and acceptor atoms, in addition to the transferring proton, using 32 beads resulted in similar QM correction difference between proton and deuteron transfer of 1.04 kcal/mol.

Thus, the current results indicate that approximately 32 beads are required to obtain reliable QM corrections to a classical PMF when using the QCP method. This is true also when computing KIE. Furthermore, to accurately compute QM corrections to a classical PMF, it is desirable to quantize the donor and acceptor atoms directly involved in the reaction, in addition to the transferring light particle. Similar findings have been observed in a previous study of the proton-transfer reaction of acetylacetone by Hinsen and Roux[53] and of malonaldehyde by Tuckerman and Marx.[52] Although we have not made a direct comparison, the efficiency of the present bisection sampling scheme should be similar to the staging approach described by Sprik et al.[21,26,58] Although the current study demonstrates that to obtain accurate KIE, it is sufficient to quantize the transferred particle alone, this is likely to be system dependent. In other systems possessing more extensive tunneling than what was observed for the current systems, multidimensional QM effects may be of importance.

Conclusions

The nuclear quantum mechanical effects in two aqueous solution proton-transfer reactions were investigated by a hybrid approach, combining QM/MM MD umbrella sampling simulations with the Quantized Classical Path (QCP) method described by Warshel and co-workers. The QCP method was augmented by the bisection algorithm (BQCP) to sample the free particle distribution and was shown to perform considerably better than when using the standard Metropolis method to sample the ring polymer chain. A sampling scheme was suggested that comprises a practical compromise between accuracy and computational cost. Additionally, different numbers of beads were tested, and the optimal choice for the systems studied was 32 beads. The conclusions found herein will be important for future studies of enzymatic reactions.

Acknowledgment. This work has been supported by the National Institutes of Health, and D.T.M. and M.G.-V. are Fulbright Scholars.

References

(1) Gao, J.; Truhlar, D. G. *Annu. Rev. Phys. Chem.* **2002**, *53*, 467−505.

(2) Garcia-Viloca, M.; Gao, J.; Karplus, M.; Truhlar, D. G. *Science* **2004**, *303*, 186−195.

(3) Benkovic, S. J.; Hammes-Schiffer, S. *Science* **2003**, *301*, 1196−1202.

(4) Kohen, A.; Limbach, H. H., Eds. *Isotope Effects in Chemistry and Biology*; Taylor & Francis Group, CRC Press: New York, 2005.

(5) Cha, Y.; Murray, C. J.; Klinman, J. P. *Science* **1989**, *243*, 1325−1330.

(6) Kohen, A.; Cannio, R.; Bartolucci, S.; Klinman, J. P. *Nature* **1999**, *399*, 496−499.

(7) Basran, J.; Sutcliffe, M. J.; Scrutton, N. S. *Biochemistry* **1999**, *38*, 3218−3222.

(8) Faulder, P. F.; Tresadern, G.; Chohan, K. K.; Scrutton, N. S.; Sutcliffe, M. J.; Hillier, I. H.; Burton, N. A. *J. Am. Chem. Soc.* **2001**, *123*, 8604−8605.

(9) Alhambra, C.; Corchado, J.; Sanchez, M. L.; Garcia-Viloca, M.; Gao, J.; Truhlar, D. G. *J. Phys. Chem. B* **2001**, *105*, 11326−11340.

(10) Billeter, S. R.; Webb, S. P.; Agarwal, P. K.; Iordanov, T.; Hammes-Schiffer, S. *J. Am. Chem. Soc.* **2001**, *123*, 11262−11272.

(11) Alhambra, C.; Luz Sanchez, M.; Corchado, J.; Gao, J.; Truhlar, D. G. *Chem. Phys. Lett.* **2001**, *347*, 512−518.

(12) Cui, Q.; Elstner, M.; Karplus, M. *J. Phys. Chem. B* **2002**, *106*, 2721−2740.

(13) Garcia-Viloca, M.; Alhambra, C.; Truhlar, D. G.; Gao, J. *J. Chem. Phys.* **2001**, *114*, 9953−9958.

(14) Tresadern, G.; Nunez, S.; Faulder, P. F.; Wang, H.; Hillier, I. H.; Burton, N. A. *Faraday Discuss.* **2002**, *122*, 223−242.

(15) Hwang, J. K.; Warshel, A. *J. Phys. Chem.* **1993**, *97*, 10053−10058.

(16) Hwang, J.-K.; Warshel, A. *J. Am. Chem. Soc.* **1996**, *118*, 11745−11751.

(17) Feierberg, I.; Luzhkov, V.; Aqvist, J. *J. Biol. Chem.* **2000**, *275*, 22657−22662.

(18) Major, D. T.; Gao, J. *J. Mol. Graphics Modell.* **2005**, *24*, 121−127.

(19) Ceperley, D. M. *Rev. Mod. Phys.* **1995**, *67*, 279−355.

(20) Ceperley, D. M.; Pollock, E. L. *Phys. Rev. Lett.* **1986**, *56*, 351−354.

(21) Sprik, M.; Klein, M. L.; Chandler, D. *Phys. Rev. B: Condens. Matter Mater. Phys.* **1985**, *31*, 4234−4244.

(22) Keirstead, W. P.; Wilson, K. R.; Hynes, J. T. *J. Chem. Phys.* **1991**, *95*, 5256−5267.

(23) Voth, G. A.; Chandler, D.; Miller, W. H. *J. Chem. Phys.* **1989**, *91*, 7749−7760.

(24) Gillan, M. J. *J. Phys. Chem. A* **1987**, *20*, 3621.

(25) Chakrabarti, N.; Carrington, T., Jr.; Roux, B. *Chem. Phys. Lett.* **1998**, *293*, 209−220.

(26) Marx, D.; Tuckerman, M. E.; Martyna, G. J. *Comput. Phys. Comm.* **1999**, *118*, 166−184.

(27) Mielke, S. L.; Truhlar, D. G. *Chem. Phys. Lett.* **2003**, *378*, 317−322.

(28) Hwang, J. K.; Chu, Z. T.; Yadav, A.; Warshel, A. *J. Phys. Chem.* **1991**, *95*, 8445−8448.

(29) Hwang, K. Y.; Cho, C.-S.; Kim, S. S.; Sung, H.-C.; Yu, Y. G.; Cho, Y. *Nature Struct. Biol.* **1999**, *6*, 422−426.

(30) Olsson, M. H. M.; Siegbahn, P. E. M.; Warshel, A. *J. Am. Chem. Soc.* **2004**, *126*, 2820−2828.

(31) Feynman, R. P.; Hibbs, A. R. *Quantum Mechanics and Path Integrals*; McGraw-Hill: New York, 1965.

(32) Voth, G. A. *Adv. Chem. Phys.* **1996**, *93*, 135−218.

(33) Pollock, E. L.; Ceperley, D. M. *Phys. Rev. B: Condens. Matter Mater. Phys.* **1984**, *30*, 2555−2568.

(34) Levy, P. *Compos. Math.* **1939**, *7*, 283.

(35) Press: W. H.; Flannery, B. P.; Teukolsky, S. A.; Vetterling, W. T. *Numerical Recipes*; University of Cambridge: New York, NY, 1992.

(36) Brooks, B. R.; Bruccoleri, R. E.; Olafson, B. D.; States, D. J.; Swaminathan, S.; Karplus, M. *J. Comput. Chem.* **1983**, *4*, 187.

(37) Jorgensen, W. L.; Chandrasekhar, J.; Madura, J. D.; Impey, R. W.; Klein, M. L. *J. Chem. Phys.* **1983**, *79*, 926−935.

(38) Gao, J. In *Rev. Comput. Chem.*; Lipkowitz, K. B., Boyd, D. B., Eds.; VCH: New York, 1995; Vol. 7, pp 119−185.

(39) Gao, J.; Thompson, M. A. *Combined Quantum Mechanical and Molecular Mechanical Methods*; American Chemical Society: Washington, DC, 1998; Vol. 712.

(40) Gao, J.; Xia, X. *Science* **1992**, *258*, 631−635.

(41) Bentzien, J.; Muller, R. P.; Florian, J.; Warshel, A. *J. Phys. Chem. B* **1998**, *102*, 2293−2301.

(42) Field, M. J.; Bash, P., A.; Karplus, M. *J. Comput. Chem.* **1990**, *11*, 700−733.

(43) Giese, T. J.; Sherer, E. C.; Cramer, C. J.; York, D. M. *J. Chem. Theory Comput.* **2005**, *1*, 1275−1285.

(44) Curtiss, L. A.; Raghavachari, K.; Redfern, P. C.; Rassolov, V.; Pople, J. A. *J. Chem. Phys.* **1998**, *109*, 7764−7776.

(45) Major, D. T.; York, D. M.; Gao, J. *J. Am. Chem. Soc.* **2005**, *127*, 16374−5.

(46) Nam, K.; Gao, J.; York, D. M. *J. Chem. Theory Comput.* **2005**, *1*, 2−13.

(47) Allen, M. P.; Tildesley, D. J. *Computer Simulation of Liquids*; Oxford University Press: Oxford, 1987.

(48) Valleau, J. P.; Torrie, G. M. In *Modern Theoretical Chemistry*; Berne, B. J., Ed.; Plenum: New York, 1977; Vol. 5, pp 169−194.

(49) Rajamani, R.; Naidoo, K.; Gao, J. *J. Comput. Chem.* **2003**, *24*, 1775−1781.

(50) Kumar, S.; Bouzida, D.; Swendsen, R. H.; Kollman, P. A.; Rosenberg, J. M. *J. Comput. Chem.* **1992**, *13*, 1011.

(51) Gao, J. *Int. J. Quantum Chem.: Quantum Chem. Symp.* **1993**, *27*, 491−499.

(52) Tuckerman, M. E.; Marx, D. *Phys. Rev. Lett.* **2001**, *86*, 4946−4949.

(53) Hinsen, K.; Roux, B. *J. Chem. Phys.* **1997**, *106*, 3567−3577.

(54) Chuang, Y.-Y.; Cramer, C. J.; Truhlar, D. G. *Int. J. Quantum Chem.* **1998**, *70*, 887−896.

(55) Valley, M. P.; Fitzpatrick, P. F. *J. Am. Chem. Soc.* **2004**, *126*, 6244−6245.

(56) Fitzpatrick, P. F.; Orville, A. M.; Nagpal, A.; Valley, M. P. *Arch. Biochem. Biophys.* **2005**, *433*, 157−165.

(57) Valley, M. P.; Fitzpatrick, P. F. *J. Am. Chem. Soc.* **2003**, *125*, 8738−8739.

(58) Martyna, G. J.; Hughes, A.; Tuckerman, M. E. *J. Chem. Phys.* **1999**, *110*, 3275−3290.

CT050257T